Dong et al., http://www.jcb.org/cgi/content/full/jcb.201304076/DC1

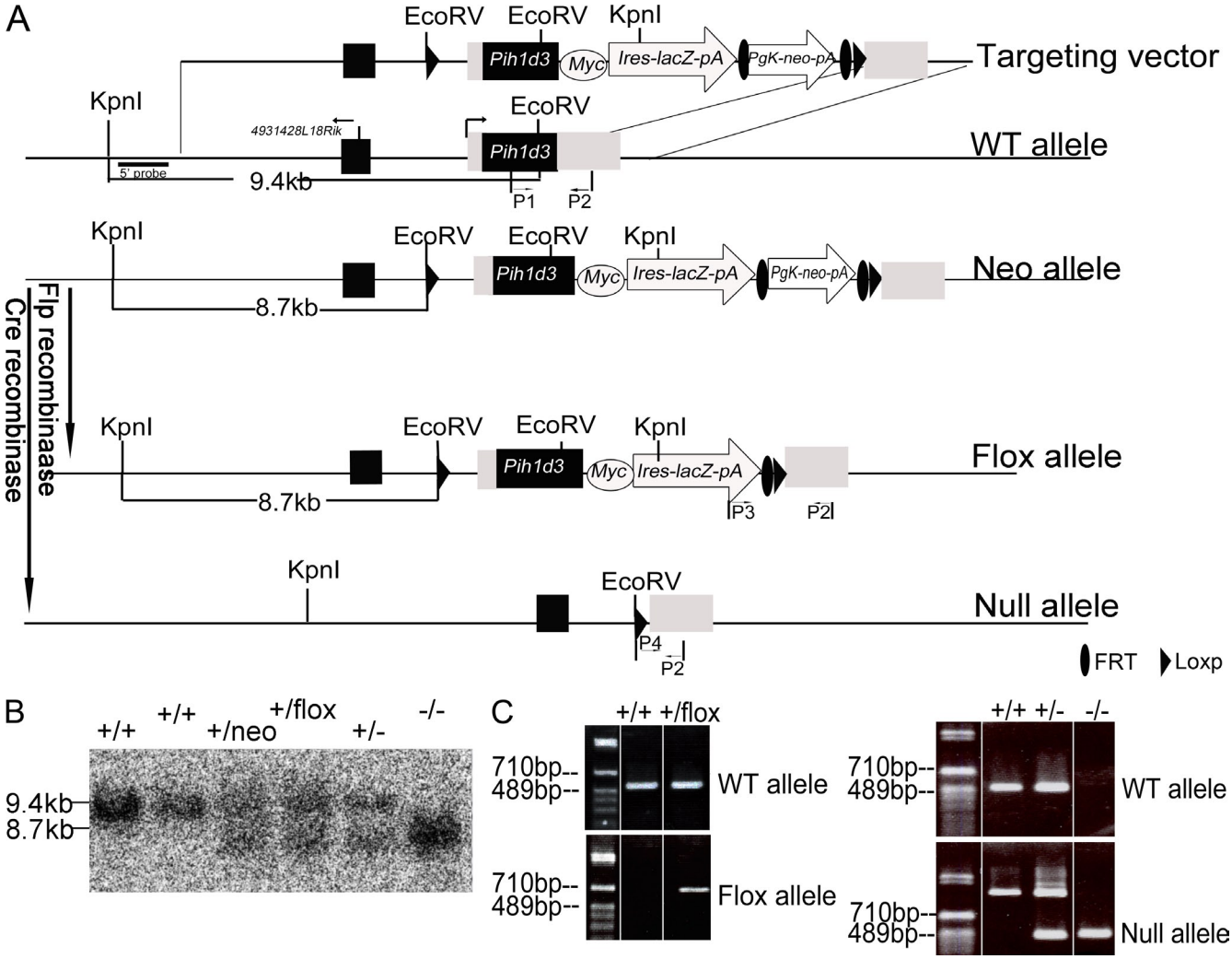

Figure S1. **Strategy for generation of *Pih1d3*$^{-/-}$ mice.** (A) Structure of the targeting vector as well as of the WT, *neo*, flox, and null alleles. The *Pih1d3* gene contains one exon (black box). In the targeting vector, the *Pih1d3* exon is followed by a Myc epitope tag sequence, an internal ribosome entry site (*Ires*)–*lacZ* ORF expression cassette, and an FRT-flanked phosphoglycerate kinase gene (*Pgk*) promoter–neomycin resistance gene (*neo*) cassette, all of which are flanked by LoxP sites. The targeting vector was integrated into the mouse genome by homologous recombination to generate the *neo* allele, the *neo* cassette of which was removed with Flp recombinase to yield the flox allele or the LoxP-flanked cassette of which was removed with Cre recombinase to yield the null allele. Diagnostic restriction enzymes (KpnI, EcoRV), a probe for Southern blot analysis (5′ probe), and primers for PCR analysis are indicated. (B) Southern blot analysis of *Pih1d3* mutant mice. Genomic DNA isolated from mice of the indicated genotypes was digested with KpnI and EcoRV and subjected to hybridization with the 5′ probe. The 9.4- and 8.7-kb bands correspond to the WT allele and to the *neo*, flox, or null alleles, respectively. (C) PCR analysis of genomic DNA from *Pih1d3* mutant mice. Primers P1 and P2 were used for detection of the WT allele (555 bp) in the left top and right top panels. Primers P3 and P2 were used to detect the flox allele (600 bp) in the bottom left panel. Primers P4 and P2 detected the null allele (444bp) and the WT allele (1272 bp) in the bottom right panel. The 555-, 600-, and 444-bp PCR products correspond to the WT, flox, and null alleles, respectively. White lines indicate the removal of intervening lanes for presentation purposes.

THE JOURNAL OF CELL BIOLOGY

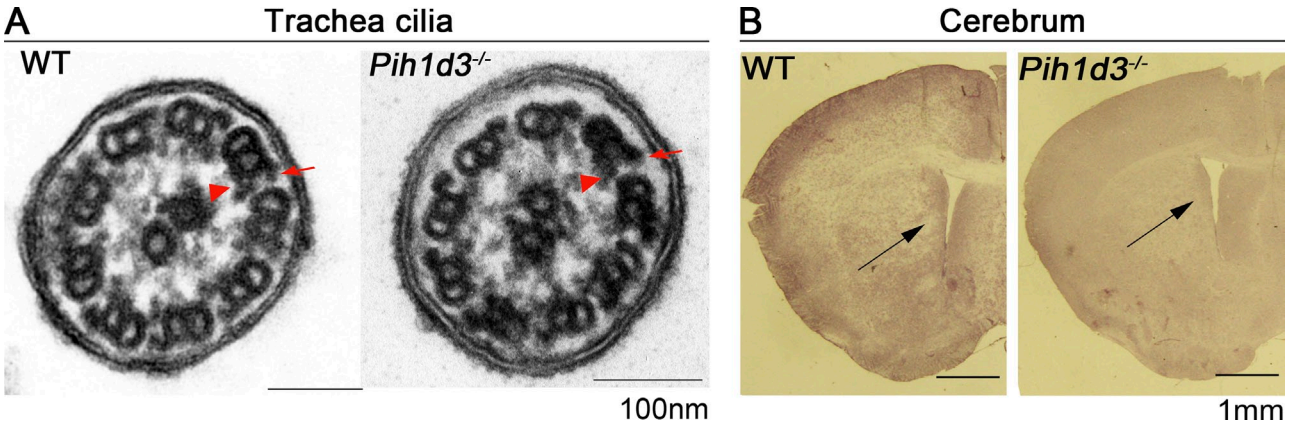

Figure S2. **Motile cilia in the trachea and brain of *Pih1d3*$^{-/-}$ mouse.** (A) TEM of cross section of trachea cilia recovered from adult WT and *Pih1d3*$^{-/-}$ mice. Arrows, outer dynein arms; arrowheads, inner dynein arms. Bar, 100 nm. (B) H&E-stained frozen sections of the cerebrum from adult WT and *Pih1d3*$^{-/-}$ mice. Arrow, the lateral ventricle. Bar, 1 mm.

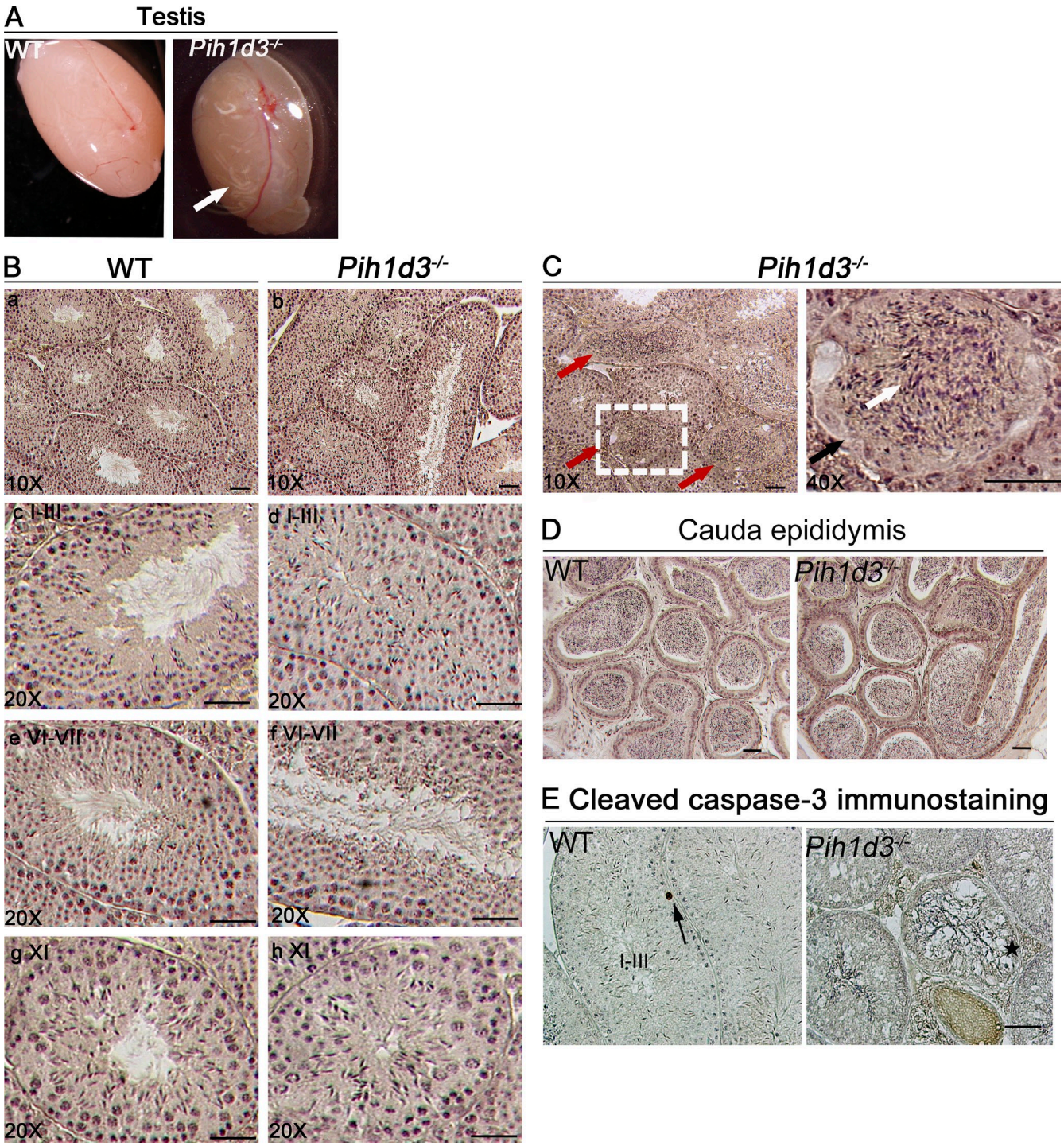

Figure S3. **Spermatogenesis in seminiferous tubules of *Pih1d3*$^{-/-}$ mice.** (A) Gross appearance of the testis of adult WT and *Pih1d3*$^{-/-}$ mice. A few seminiferous tubules of the *Pih1d3*$^{-/-}$ testis appear abnormal (arrow). (B and C) H&E staining of the testis of adult WT and *Pih1d3*$^{-/-}$ mice. Stages of the cycle of the seminiferous epithelium are indicated with roman numerals. Whereas spermatogenesis appeared to proceed normally in most seminiferous tubules of the mutant (B), some seminiferous tubules (C, red arrows) appeared abnormal. Higher magnification (40×) of the boxed region in the left panel of C is shown in the right panel. Spermatogenetic cells, which are normally located near the basal lamina of the seminiferous tubules, are lost in the tubules (black arrow), while elongated spermatids accumulate in the lumen (white arrow). Bars, 50 µm. (D) H&E staining of the cauda epididymis of adult WT and *Pih1d3*$^{-/-}$ mice. The cauda epididymis of the mutant appeared normal. Bars, 50 µm. (E) Immunochemical staining of the testis of adult WT and *Pih1d3*$^{-/-}$ mice with antibodies to the cleaved form of caspase-3. The arrow indicates an apoptotic cell (brown immunoreactivity), whereas the asterisk denotes abnormal seminiferous tubules in the mutant. Bar, 50 µm.

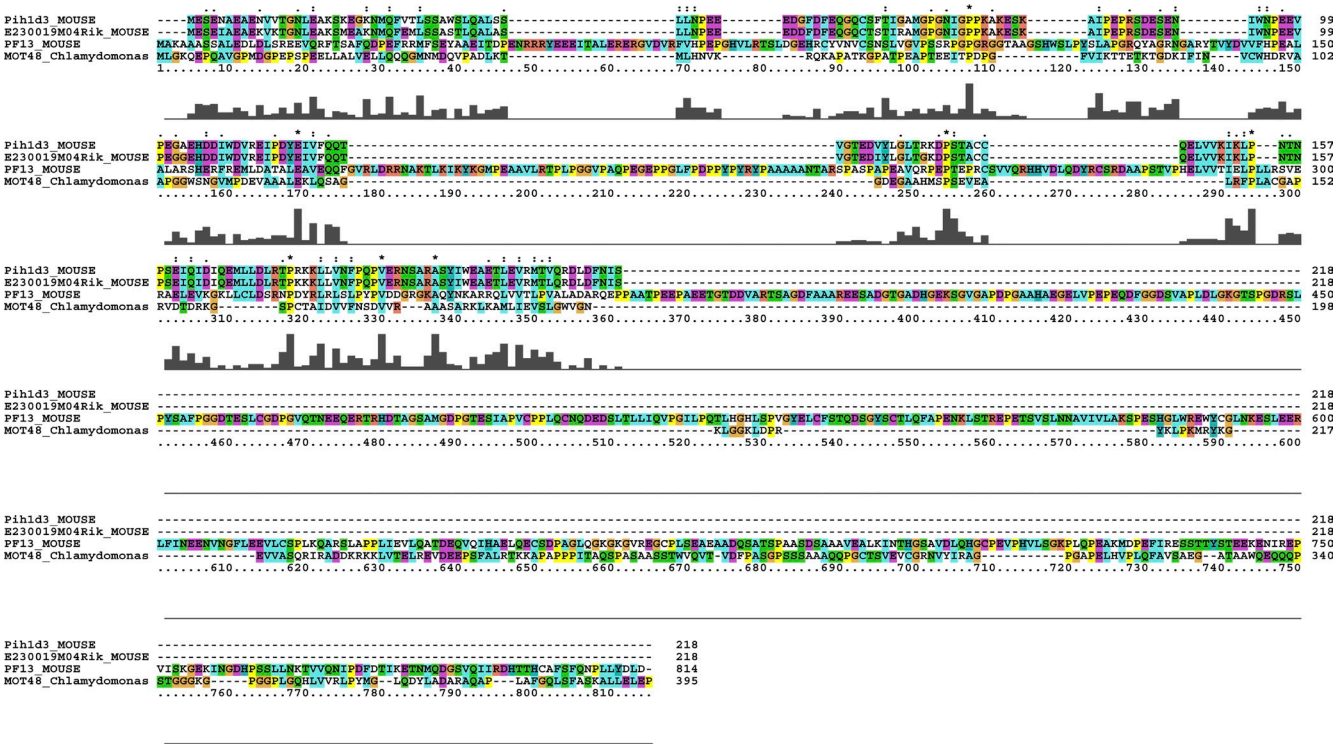

Figure S4. **Amino acid sequence alignment of four PIH1 proteins.** Protein sequence of four PIH1 proteins, Pih1d3 (mouse), E230019M04Rik (mouse), Dnaaf1/Pf13 (mouse), and MOT48 (*Chlamydomonas*), were aligned using Clustal X software.

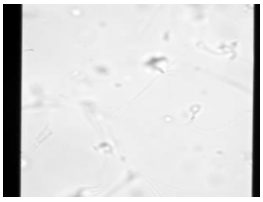

Video 1. **Movie of WT sperm.** Motility of WT sperm was examined by EMCCD camera (iXon+; Andor Technology) with a halogen lamp via an intravital microscope (AF DMI 6000B; Leica). The images were captured at 30 frames/s during 5 s. WT sperm were motile.

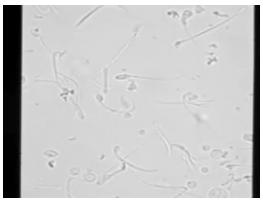

Video 2. **Movie of *Pih1d3*$^{-/-}$ sperm.** Motility of *Pih1d3*$^{-/-}$ sperm was examined by EMCCD camera (iXon+; Andor Technology) with a halogen lamp via an intravital microscope (AF DMI 6000B; Leica). The images were captured at 30 frames/s during 5 s. The *Pih1d3*$^{-/-}$ sperm were immotile.

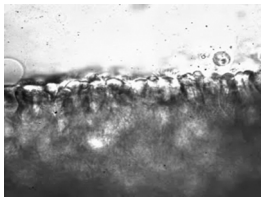

Video 3. **Movie of WT trachea cilia.** Motility of trachea cilia in WT mice was examined by a high speed camera (HAS-500; Detect) with a halogen lamp via an upright microscope (AxioPlan2; Carl Zeiss). The images were captured at 100 frames/s during 2 s. Note that trachea cilia were motile in WT mice.

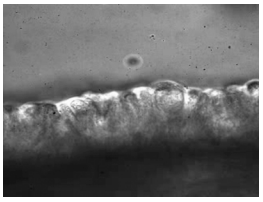

Video 4. **Movie of *Pih1d3*$^{-/-}$ trachea cilia.** Motility of trachea cilia in *Pih1d3*$^{-/-}$ mice was examined by a high speed camera (HAS-500; Detect) with a halogen lamp via an upright microscope (AxioPlan2; Carl Zeiss). The images were captured at 100 frames/s during 2 s. Note that trachea cilia were motile in *Pih1d3*$^{-/-}$ mice.

Table S1. **Testis weight and sperm numbers in WT and *Pih1d3*$^{-/-}$ mice**

	Testis weight (mg)		Sperm number (× 10^6, per cauda epididymis)	
	WT	***Pih1d3*$^{-/-}$**	**WT**	***Pih1d3*$^{-/-}$**
	86.9	84.8	6.56	4.32
	87.6	82.1	8.66	4.18
	86.8	85.5	7.05	4.49
	83.1	84.6	6.27	4.54
	83.3	84.8	9.38	4.29
	86.2	89.7	8.26	4.35
Average	86.00 ± 0.46	85.25 ± 0.64	8.22 ± 0.36	4.26 ± 0.05
P value	>0.05		<0.01	

Three WT mice (8 wk) and three *Pih1d3*$^{-/-}$ mice (8 wk) were examined for the weight of the testis and the number of sperm stored in the cauda epididymis. For each mouse, the two testes were measured for both. There was no significant difference in the weight between WT and *Pih1d3*$^{-/-}$ testes ($P > 0.05$). The number of mature sperm stored in the cauda epididymis was reduced in *Pih1d3*$^{-/-}$ mice ($P < 0.01$). Data are means ± SEM ($n = 3$).

Table S2. **Percentage of abnormal seminiferous tubules in *Pih1d3*$^{-/-}$ mice**

***Pih1d3*$^{-/-}$**	**Abnormal**	**Total**	**Percentage**	**Average percentage**
	7	189	3.70	
1#	6	161	3.73	3.84
	6	147	4.1	
	8	176	4.54	
2#	8	183	4.37	4.22
	7	187	3.74	
	10	212	4.32	
3#	8	174	4.59	4.41
	7	179	3.91	
Abnormal/total (%)				4.16 ± 0.10

Numbers of the abnormal seminiferous tubules in *Pih1d3*$^{-/-}$ mice were counted by observing H&E-stained cross sections of *Pih1d3*$^{-/-}$ testis. Sections of three testes from three independent *Pih1d3*$^{-/-}$ mice were observed. For one *Pih1d3*$^{-/-}$ testis, three sections from different regions of the testis were analyzed. Data are means ± SEM ($n = 3$).